

A Rain Drop Size Distribution (DSD) Retrieval Algorithm for CASA DFW Urban Radar Network

Haonan Chen¹, V. Chandrasekar¹, and Eiichi Yoshikawa²

¹Colorado State University, Fort Collins, CO, USA

²Japan Aerospace Exploration Agency (JAXA), Tokyo, Japan

ABSTRACT

The raindrop size distribution (RSD) is a fundamental descriptor of rain microphysics, and hence extensive effort has been under way to measure RSD through both in-situ sampling devices as well as remote observations. The raindrop size distribution along with shape information, essentially determines the behavior of dual polarization observations of precipitation. A remote estimator of RSD from radar observation significantly enhances the area over which RSD is observed. The Dallas-Fort Worth urban demonstration radar network is being implemented by the Center for Collaborative Adaptive Sensing of Atmosphere (CASA), as a demonstration of the X-band radar network concept in a metropolitan region. Though it is an operational radar network, it provides great opportunity to study the RSD variability over different types of storms for scientific applications. This paper will implement and evaluate various RSD estimation techniques using data collected from NEXRAD in DFW region as well as the dual-frequency CSU-CHILL radar.

Index Terms --- CASA, DFW network, X-band radar, dual-polarization, raindrop size distribution (RSD)

1. INTRODUCTION

In recent years, there is an increasing interest in the use of X-band weather radars because of the cost efficiency and ability to shoot sensitive areas that are inadequately covered by operational S-band radar network. The concepts and principles of X-band radar network introduced by the National Science Foundation (NSF)'s Engineering Research Center (ERC) for Collaborative Adaptive Sensing of the Atmosphere (CASA) have shown great advantages to observe low-level atmospheric phenomena such as tornadoes and flash flood (Chandrasekar et al. 2004). The center has been pursuing an innovative radar networking paradigm to overcome the coverage and resolution limitations of the National Weather Services (NWS) Weather Surveillance Radar-1988 Doppler (WSR-88D) network. This Distributed Collaborative Adaptive Sensing (DCAS)

paradigm was validated and evaluated in the prototype of such kind of network deployed in Southwestern Oklahoma, which demonstrated the success of CASA radar network in terms of meteorological command and control, networked product retrieval, quantitative precipitation estimation (QPE), tornado tracking, vector wind retrieval, and nowcasting (Chandrasekar et al. 2010).

From 2012, CASA, in collaboration with the North Central Texas Council of Governments (NCTCOG) started to establish the first urban weather radar remote sensing network in Dallas-Fort Worth (DFW) metroplex to demonstrate the DCAS concepts. The main goal is to protect the safety and prosperity of humans and ecosystems through creating high-resolution, three-dimensional mapping of the meteorological conditions and helping the local emergency managers issue impacts-based warnings and forecasts for severe wind, tornadoes, and flash flood hazards (Chandrasekar et al. 2013). Radar QPE is one of the major research activities in the development of this urban network (Chen and Chandrasekar, 2012). As building blocks for deriving physically based radar rainfall algorithms, the understanding of variability of raindrop size distribution (RSD) is an important topic in hydrometeorological research. Many studies have been done to estimate the parameters of a gamma RSD model using polarimetric radar observations at S-band (Bringi et al. 2002, Gorgucci et al. 2002). However, most of the research was focusing on the S-band data or the simulation data based on the S-band radar observations. This paper will implement and evaluate various RSD estimation techniques using real data collected from the NEXRAD in DFW region and data collected by the dual-frequency CSU-CHILL radar.

This paper is organized as follows. In section 2, a review of gamma RSD model and the implication of RSD on polarimetric radar measurements will be presented. The algorithms used to estimate the two main RSD parameters, namely, D_0 and N_w , based on the dual-polarization radar observations are described in section 3. Sample results for real data implementation will be given in section 4, followed by a brief discussion of future work in section 5.

* Corresponding author address: Haonan Chen, 1373 Campus Delivery, Colorado State University, Fort Collins, CO 80523; e-mail: Haonan.Chen@colostate.edu

2. RAINDROP SIZE DISTRIBUTION (RSD) AND ITS IMPLICATION FOR DUAL-POLARIZATION RADAR MEASUREMENTS

The raindrop size distribution describes the probability density distribution function of raindrop sizes. A good knowledge of the RSD in the precipitating system is necessary for accurate radar QPE and QPF. Since the early work of Marshall and Palmer (1948), various DSD models have been proposed, among which the gamma distribution model can adequately represent many of the natural variations in the shape of the raindrop size distribution (Ulbrich 1983). The corresponding form of gamma DSD can be expressed as:

$$N(D) = N_0 D^\mu e^{-\Lambda D} \quad (1)$$

where N_0 is the intercept parameter in $m^{-3}mm^{-1-\mu}$, μ is a distribution shape parameter, Λ is a slope term in mm^{-1} , and D is the volume equivalent diameter in mm. The raindrop size distribution model used in this study is the "normalized" gamma distribution (Testud et al. 2000) that can be described as:

$$N(D) = N_w f(\mu) \left(\frac{D}{D_0}\right)^\mu \exp\left[-(3.67 + \mu)\frac{D}{D_0}\right] \quad (2)$$

where N_w is the scaled version of N_0 defined as:

$$N_w = \frac{N_0}{f(\mu)} D_0^\mu \quad (3)$$

$$f(\mu) = \frac{6}{(3.67)^\mu} \cdot \frac{(3.67 + \mu)^{\mu+4}}{\Gamma(\mu+4)} \quad (4)$$

Obviously, N_w , D_0 , and μ are the three parameters of the gamma DSD.

The dual-polarization radar measurements, namely, reflectivity at horizontal polarization (Z_h) and vertical polarization (Z_v), differential reflectivity (Z_{dr}), and specific differential phase (K_{dp}), can be related to the integral form of drop size distribution as:

$$Z_h = \frac{\lambda^4}{\pi^5 |K_w|^2} \int \sigma_h(D) N(D) dD \quad (5)$$

$$Z_v = \frac{\lambda^4}{\pi^5 |K_w|^2} \int \sigma_v(D) N(D) dD \quad (6)$$

$$Z_{dr} = 10 \log_{10} \frac{Z_h}{Z_v} = 10 \log_{10} \left(\frac{\int \sigma_h(D) N(D) dD}{\int \sigma_v(D) N(D) dD} \right) \quad (7)$$

$$K_{dp} = \frac{180}{\pi} \lambda \operatorname{Re} \int [f_h(D) - f_v(D)] N(D) dD \quad (8)$$

where λ is the radar wavelength, σ_h and σ_v are the radar cross section at horizontal and vertical polarization, respectively, K_w is the dielectric factor of water given by $K_w = (\epsilon_r - 1)/(\epsilon_r + 2)$, here ϵ_r is the complex dielectric constant of water, f_h and f_v are the complex forward-

scatter amplitudes at horizontal and vertical polarizations, respectively.

3. DESCRIPTION OF THE RSD PARAMETER RETRIEVAL ALGORITHMS

In this section, the dual-polarization observation based RSD parameter retrieval algorithms will be described in details.

3.1. RETRIEVAL ALGORITHMS FOR S-BAND RADAR

The RSD retrieval algorithm for S-band radar used in this paper is based on a modified version of the " β " method proposed by Gorgucci et al. (2002). It takes account of three dual-polarization observations include Z_h (in dBZ), Z_{dr} (in dB), and K_{dp} (in deg/km).

If $Z_h \geq 35$ dBZ, $Z_{dr} > 0.2$ dB, $K_{dp} > 0.3$ deg/km, D_0 and N_w are retrieved as:

$$\beta = 2.08 Z_{hL}^{-0.365} K_{dp}^{0.38} Z_{drL}^{0.965} \quad (9)$$

$$D_0 = a_1 Z_{hL}^{b_1} Z_{drL}^{c_1} \quad (10)$$

where $Z_{hL} = 10^{Z_h/10}$, and $Z_{drL} = 10^{Z_{dr}/10}$ are reflectivity and differential reflectivity in linear unit. And the coefficients are $a_1 = 0.595\beta^{0.0353}$, $b_1 = 0.0242\beta^{-0.359}$, $c_1 = 0.103\beta^{-0.91}$.

$$\log_{10} N_w = a_2 Z_{hL}^{b_2} Z_{drL}^{c_2} \quad (11)$$

with coefficients as $a_2 = 3.12\beta^{0.0201}$, $b_2 = 0.176\beta^{0.376}$, $c_2 = -0.101\beta^{-0.897}$.

If $Z_h < 35$ dBZ, $Z_{dr} \geq 0.2$ dB,

$$D_0 = 1.81 Z_{dr}^{0.486} \quad (12)$$

$$N_w = \frac{21 Z_{hL}}{D_0^{7.353}} \quad (13)$$

If $Z_h < 35$ dBZ, $Z_{dr} < 0.2$ dB,

$$D_0 = 1.81 * \gamma^{0.486} * Z_{hL}^{0.136} \quad (14)$$

$$N_w = \left(\frac{1.513}{1.81 * \gamma^{0.486}} \right)^{7.35} \quad (15)$$

where $\gamma = \frac{\langle Z_{dr} \rangle}{\langle Z_{hL}^{0.37} \rangle}$.

3.2. RETRIEVAL ALGORITHMS FOR X-BAND RADAR

For RSD retrieval using X-band radar observations, we calculate the β as:

$$\beta = 0.536 (K_{dp}/Z_{hL})^{0.276} Z_{drL}^{1.212} \quad (16)$$

Then, D_0 and N_w will be retrieved as:

$$D_0 = a_1 \left(\frac{Z_{drL} - 0.8}{\beta} \right)^{b_1} \quad (17)$$

$$\log_{10} N_w = a_2 Z_{hL}^{b_2} \left(\frac{Z_{drL} - 0.8}{\beta} \right)^{c_2} \quad (18)$$

where $a_1 = 0.201$, $b_1 = 0.884$, $a_2 = 7.030$, $b_2 = 0.083$, $c_2 = 0.581$.

4. REAL DATA IMPLEMENTATION

The testing of retrieval algorithms has been performed with radar data collected by dual-frequency CSU-CHILL radar and a NEXRAD site in the DFW area. Nevertheless, instead of directly taking the radar measurements, we first apply a data quality control (QC) process because it is not an easy work to get the intrinsic values the radar should measure, especially at higher/attenuating frequency such as X-band. The principle of this QC program is based on the microphysical characteristics of precipitation with relatively high co-polar correlation and relatively smooth radial behavior of differential propagation phase. A data quality mask is generated based on the thresholds of ρ_{hv} , standard deviation of Φ_{DP} , and signal-to-noise ratio (SNR) (Wang and Chandrasekar, 2009). The quality controlled data is well suited for mitigation of non-meteorological clutter contamination. In addition, a hybrid rainfall estimation algorithm is developed to measure the rainfall rate using the masked data. But the relation between rainfall rate measurements and raindrop size distribution is beyond the scope of this paper.

Figure 1(a)(b)(c) show the fields of Z_h , Z_{dr} , and K_{dp} for KFWS radar for the rainfall event occurred in the DFW region on June 9th, 2013. Corresponding RSD retrieval results based on algorithm described in Section 3.1 are shown in Figure 2(a)(b). Figure 3(a)(b) are histograms of the distribution of D_0 and $\log_{10}(N_w)$ in the region where rainfall rate is higher than 10 mm/hr.

A strong storm passing CSU-CHILL radar observing range on August 12th, 2013 is also used to demonstrate the data mask quality and test the RSD retrieval methodologies. The fields of Z_h , Z_{dr} , and K_{dp} from CHILL S-band radar are shown in Figure 4(a)(b)(c). Figure 5(a)(b) are the RSD retrieval results. Corresponding histograms of the distribution of D_0 and $\log_{10}(N_w)$ are shown in Figure 6(a)(b). The X-band data collected by CHILL radar for the same storm event was also used, to demonstrate the X-band RSD retrieval algorithm presented in Section 3.2. Similarly, Figure 7(a)(b)(c) are the fields of Z_h , Z_{dr} , and K_{dp} for CHILL X-band data, whereas Figure 8(a)(b) show the histograms of distribution of D_0 and $\log_{10}(N_w)$ in the region where rainfall rate is higher than 10 mm/hr.

5. DISCUSSION AND FUTURE WORK

From the PPI plots and histograms of D_0 and $\log_{10}(N_w)$, we can conclude that the two RSD retrieval algorithms work fairly well especially for heavy rainfall.

However, these algorithms depend on a few assumptions on the rain drop shape mode, and the precipitation types. It is also greatly based on the data quality control process including the attenuation correction of reflectivity and differential reflectivity, and estimation of the specific differential propagation phase.

The future work will be focusing on the impacts of data quality control on the RSD algorithms, as well as the hydrometeor classification before applying any RSD parameter estimation algorithm.

ACKNOWLEDGMENTS

This research is supported by the National Science Foundation and NOAA/NWS.

REFERENCES

- Bringi, V.N., G. J. Huang, V. Chandrasekar, E. Gorgucci, 2002: A Methodology for Estimating the Parameters of a Gamma Raindrop Size Distribution Model from Polarimetric Radar Data: Application to a Squall-Line Event from the TRMM/Brazil Campaign. *J. Atmos. Oceanic Technol.*, **19**, 633–645.
- Chandrasekar, V., S. Lim, N. Bharadwaj, W. Li, D. McLaughlin, V. N. Bringi, and E. Gorgucci, 2004: Principles of networked weather radar operation at attenuating frequencies. *Proc. Third European Conf. on Radar Meteorology*, Visby, Sweden, ERAD, 109–114.
- Chandrasekar, V., and Coauthors, 2010: The CASA IP1 test-bed after 5 years operation: Accomplishments, breakthroughs, challenges and lessons learned, *Proc. of the 6th European Conf. on Radar in Meteorology and Hydrology*, Sibiu, Romania.
- Chandrasekar, V., and Coauthors, 2013: The CASA Dallas Fort Worth Remote Sensing Network ICT for Urban Disaster Mitigation, *Proc. of EGU General Assembly*, 7-12 April, Vienna, Austria.
- Chen, H., and V. Chandrasekar, 2012: High Resolution Rainfall Mapping in the Dallas-Fort Worth Urban Demonstration Network, *Proc. of International Geoscience and Remote Sensing Symposium (IGARSS2012)*, 22-27 July, Munich, Germany.
- Gorgucci, Eugenio, V. Chandrasekar, V. N. Bringi, Gianfranco Scarchilli, 2002: Estimation of Raindrop Size Distribution Parameters from Polarimetric Radar Measurements. *J. Atmos. Sci.*, **59**, 2373–2384.
- Marshall, J. S., W. Mc K. Palmer, 1948: The Distribution of Raindrops with Size. *J. Meteor.*, **5**, 165–166.
- Testud, Jacques, Erwan Le Bouar, Estelle Obligis, Mustapha Ali-Mehenni, 2000: The Rain Profiling Algorithm Applied to Polarimetric Weather Radar. *J. Atmos. Oceanic Technol.*, **17**, 332–356.
- Ulbrich, Carlton W., 1983: Natural Variations in the Analytical Form of the Raindrop Size Distribution. *J. Climate Appl. Meteor.*, **22**, 1764–1775.
- Wang, Yanting, V. Chandrasekar, 2009: Algorithm for Estimation of the Specific Differential Phase. *J. Atmos. Oceanic Technol.*, **26**, 2565–2578.

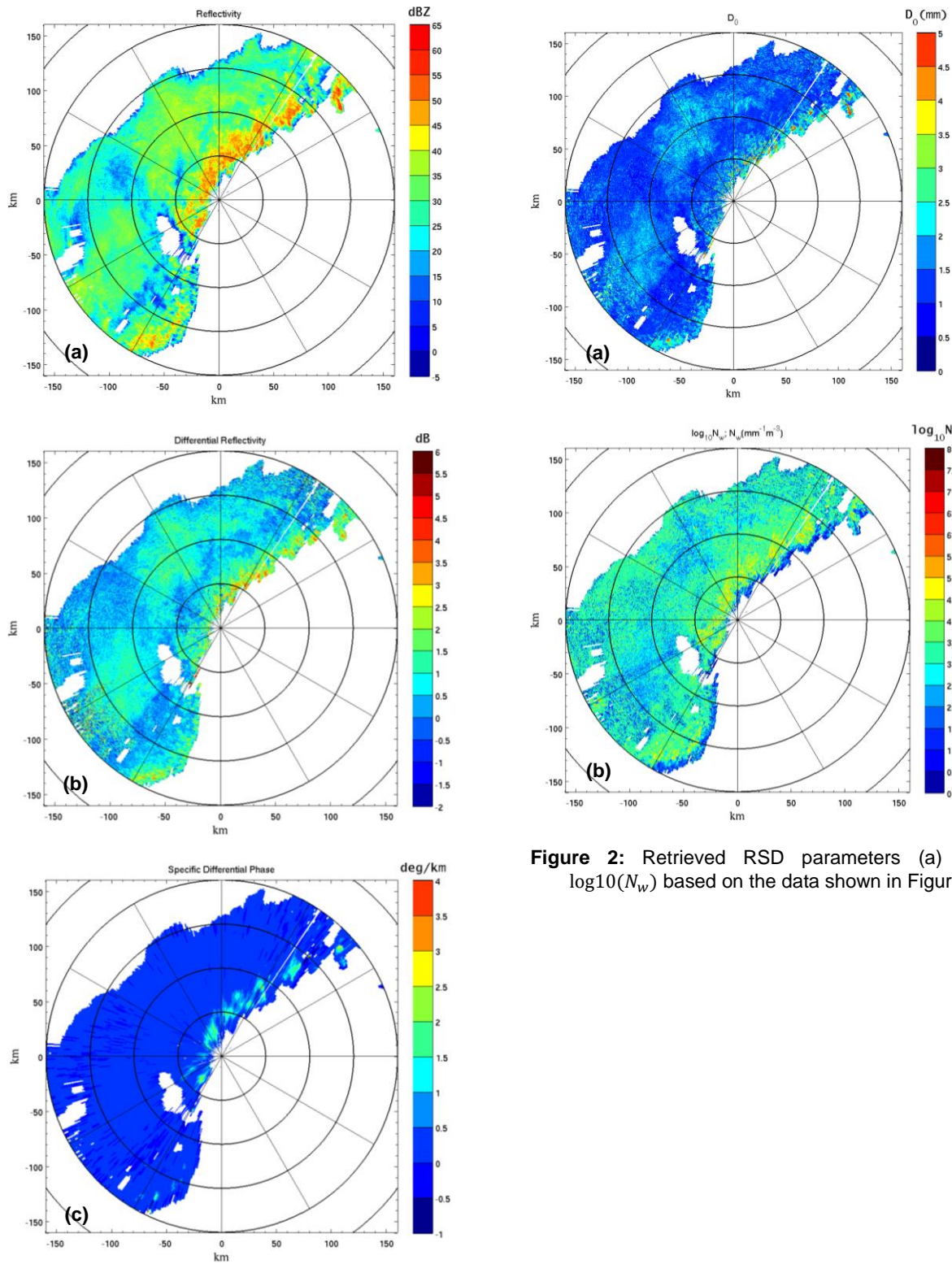


Figure 2: Retrieved RSD parameters (a) D_0 (b) $\log_{10}(N_w)$ based on the data shown in Figure 1.

Figure 1: (a) Z_h (b) Z_{dr} (c) K_{dp} fields from KFWS observations at 11:00:59UTC, June 9th, 2013.

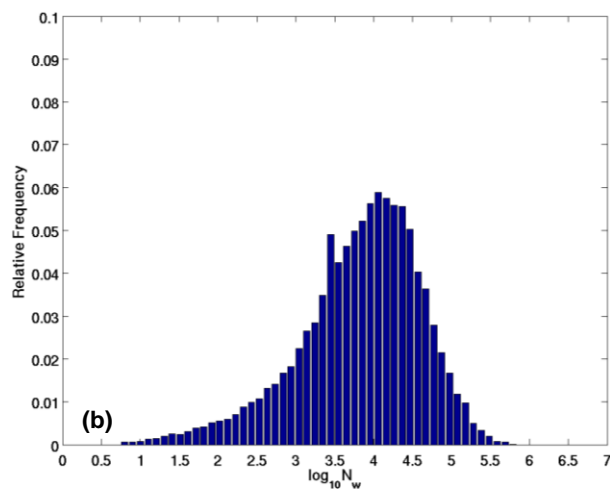
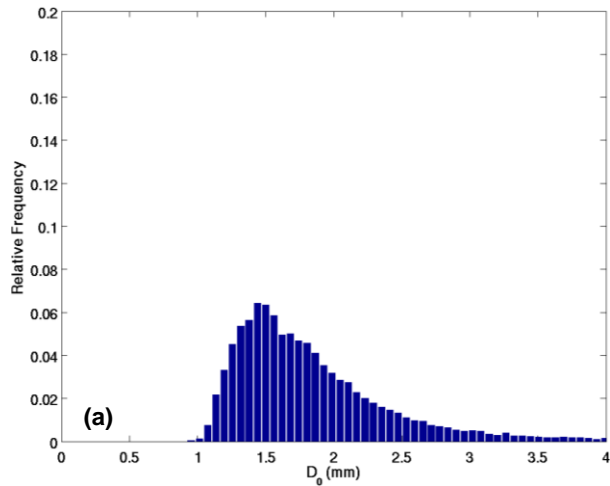


Figure 3: Histogram of the distribution of (a) D_0 (b) $\log_{10}(N_w)$ in the region where rainfall rate is higher than 10 mm/hr for the June 9th, 2013 rainfall case.

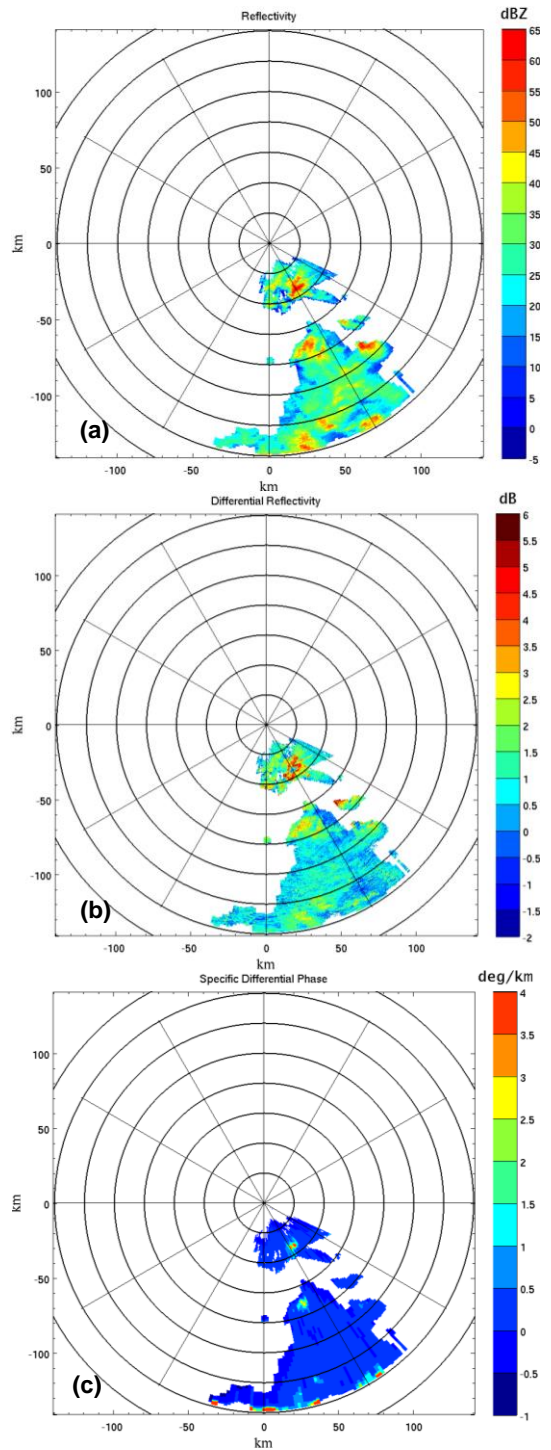


Figure 4: (a) Z_h (b) Z_{dr} (c) K_{dp} fields from CSU-CHILL S-band observations at 21:42:44UTC, Aug 12th, 2013.

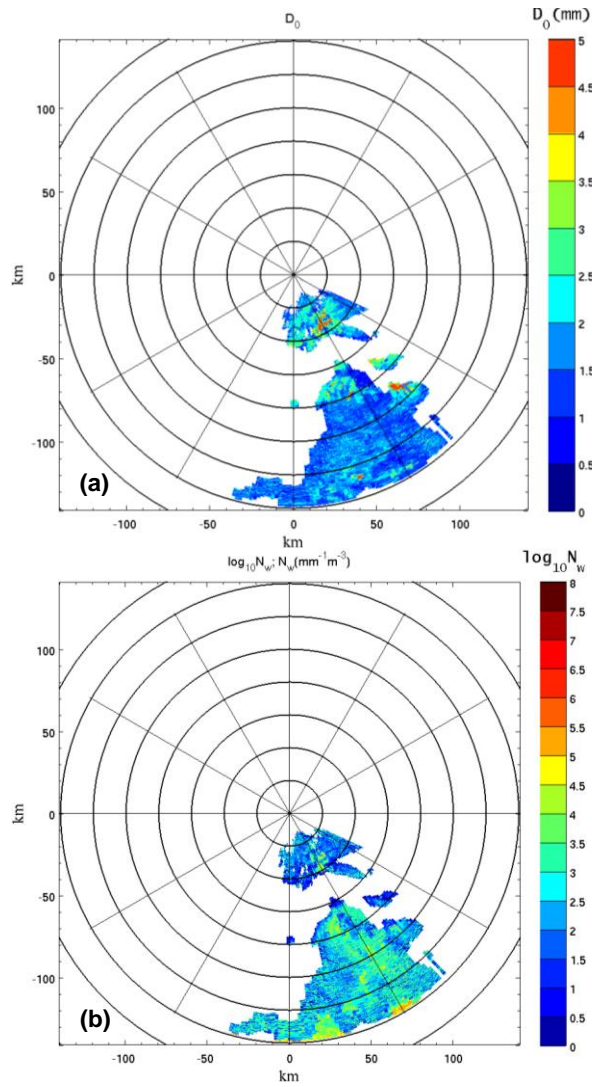


Figure 5: RSD parameters (a) D_0 (b) $\log_{10}(N_w)$ based on the data shown in Figure 4.

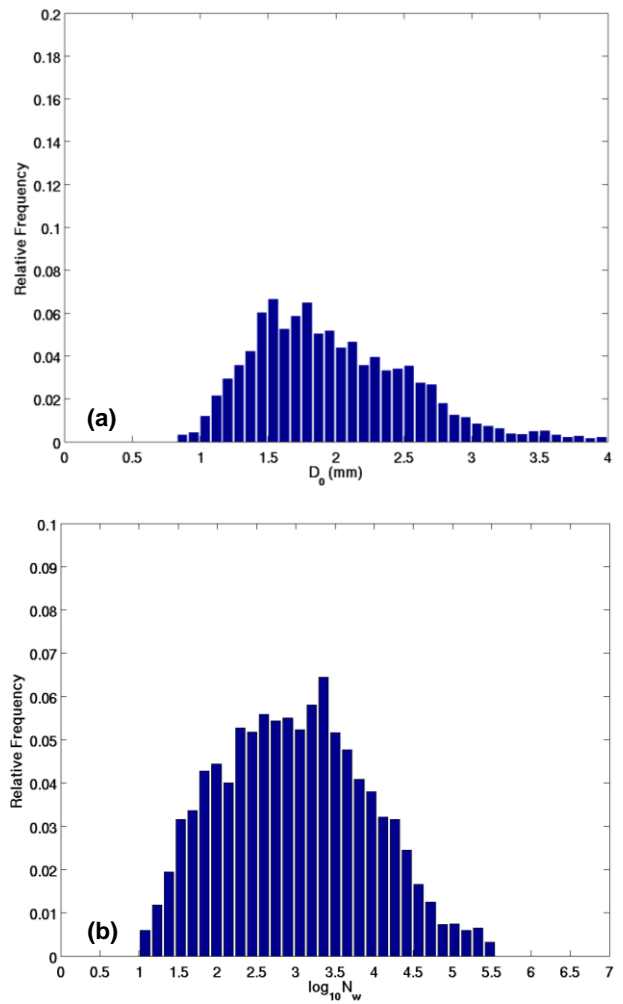


Figure 6: Histogram of the distribution of (a) D_0 (b) $\log_{10}(N_w)$ for the Aug 12th, 2013 rainfall case observed by CSU-CHILL S-band radar.

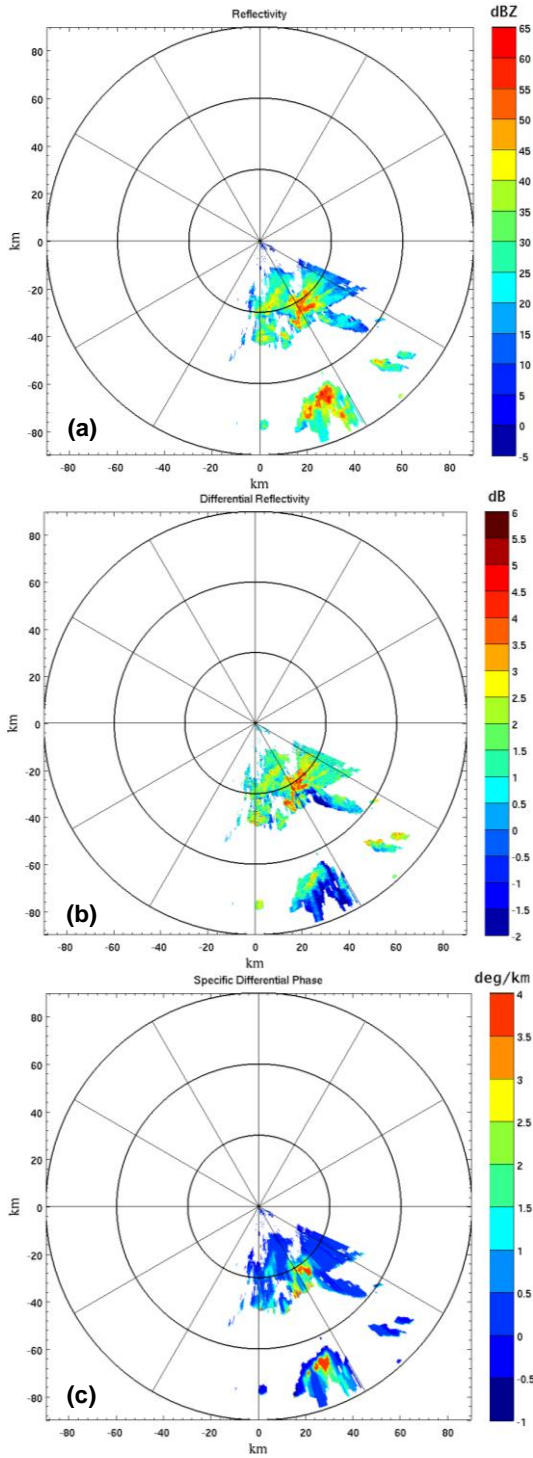


Figure 7: (a) Z_h (b) Z_{dr} (c) K_{dp} fields from CSU-CHILL X-band observations at 21:42:44UTC, Aug 12th, 2013.

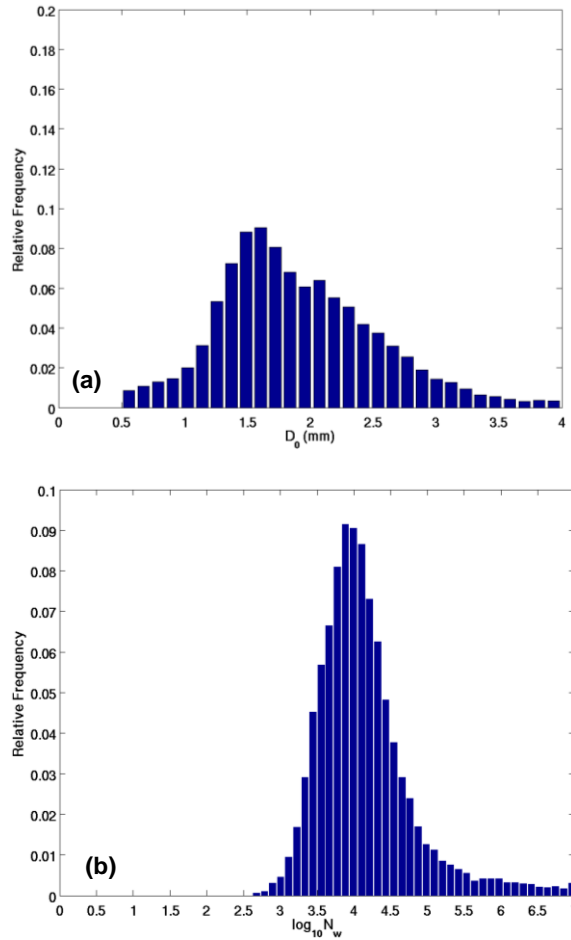


Figure 8: Histogram of the distribution of (a) D_0 (b) $\log_{10}(N_w)$ in the region where rainfall rate is higher than 10 mm/hr for the Aug 12th, 2013 rainfall case observed by CSU-CHILL X-band radar.